Journal Pre-proof

Serum phospholipidomics reveals altered lipid profile and promising biomarkers in multiple sclerosis

Helena Beatriz Ferreira, Tânia Melo, Andreia Monteiro, Artur Paiva, Pedro Domingues, M. Rosário Domingues

PII: S0003-9861(20)30681-0

DOI: https://doi.org/10.1016/j.abb.2020.108672

Reference: YABBI 108672

To appear in: *Archives of Biochemistry and Biophysics*

Received Date: 7 August 2020

Revised Date: 5 November 2020

Accepted Date: 8 November 2020

Please cite this article as: H.B. Ferreira, Tâ. Melo, A. Monteiro, A. Paiva, P. Domingues, M.Rosá. Domingues, Serum phospholipidomics reveals altered lipid profile and promising biomarkers in multiple sclerosis, *Archives of Biochemistry and Biophysics* (2020), doi: https://doi.org/10.1016/j.abb.2020.108672.

Serum phospholipidomics reveals altered lipid profile and promising biomarkers in multiple sclerosis

Helena Beatriz Ferreira[1,2], Tânia Melo[1,2], Andreia Monteiro[3,4], Artur Paiva[5,6,7], Pedro Domingues[1], M. Rosário Domingues[1,2*]

1. Mass Spectrometry Center, QOPNA/LAQV-REQUIMTE, Department of Chemistry, University of Aveiro, Campus Universitário de Santiago, 3810-193 Aveiro, Portugal

2. CESAM, Centre for Environmental and Marine Studies, Department of Chemistry, University of Aveiro, Campus Universitário de Santiago 3810-193 Aveiro, Portugal

3. Health Sciences Research Centre, Universidade da Beira Interior (CICS-UBI), Avenida Infante D. Henrique, Covilhã 6200-506, Portugal

4. Serviço Patologia Clínica, Centro Hospitalar Cova da Beira, Quinta do Alvito, 6200-251 Covilhã, Portugal

5. Unidade de Gestão Operacional em Citometria, Centro Hospitalar e Universitário de Coimbra (CHUC, Portugal).

6. Coimbra Institute for Clinical and Biomedical Research (iCBR), Faculty of Medicine, University of Coimbra, (Coimbra, Portugal).

7. Instituto Politécnico de Coimbra, ESTESC - Coimbra Health School, Ciências Biomédicas Laboratoriais (Portugal).

***Corresponding author:** M. Rosário Domingues, Chemistry Department of University of Aveiro, Campus Universitário de Santiago, 3810-193 Aveiro, Portugal. E-mail: mrd@ua.pt

Tel.:+351 234 370 698

Abstract

Multiple sclerosis is a neurodegenerative disease causing disability in young adults. Alterations in metabolism and lipid profile have been associated with this disease. Several studies have reported changes in the metabolism of arachidonic acid and the profile of fatty acids, ceramides, phospholipids and lipid peroxidation products. Nevertheless, the understanding of the modulation of circulating lipids at the molecular level in multiple sclerosis remains unclear. In the present study, we sought to assess the existence of a distinctive lipid signature of multiple sclerosis using an untargeted lipidomics approach. It also aimed to assess the differences in lipid profile between disease status (relapse and remission). For this, we used hydrophilic interaction liquid chromatography coupled with mass spectrometry for phospholipidomic profiling of serum samples from patients with multiple sclerosis. Our results demonstrated that multiple sclerosis has a phospholipidomic signature different from that of healthy controls, especially the PE, PC, LPE, ether-linked PE and ether-linked PC species. Plasmalogen PC and PE species, which are natural endogenous antioxidants, as well as PC and PE polyunsaturated fatty acid esterified species showed significantly lower levels in patients with multiple sclerosis and patients in both remission and relapse of multiple sclerosis. Our results show for the first time that the serum phospholipidome of multiple sclerosis is significantly different from that of healthy controls and that few phospholipids, with the lowest p-value, such as PC(34:3), PC(36:6), PE(40:10) and PC(38:1) may be suitable as biomarkers for clinical applications in multiple sclerosis.

Keywords: multiple sclerosis; lipidomic; mass spectrometry; lipid profile; phospholipids; plasmalogens

Abbreviations: ACN: acetonitrile; AGC: automatic gain control; AUC: areas under curve; Cer: ceramides; CHCB: Centro Hospitalar Cova da Beira; FA: fatty acids; HC: healthy controls; HCA: hierarchical clustering analysis; HILIC-MS/MS: hydrophilic interaction liquid chromatography - tandem mass spectrometry; HPLC: high-performance liquid chromatography; LC-MS: liquid chromatography-mass spectrometry; LPC: lyso-phosphatidylcholine; LPE: lyso-phosphatidylethanolamine; LPG: lyso-phosphatidylglycerol; LPI: lyso-phosphatidylinositol; MSs: multiple sclerosis; MS/MS: tandem mass spectrometry; P: phosphorus; PA: phosphatidic acid; PC: phosphatidylcholine; PCA: principal component analysis; PE: phosphatidylethanolamine; PG: phosphatidylglycerol; PI: phosphatidylinositol; PL: phospholipids; PLA2: phospholipase A2; PPARα: peroxisome proliferator-activated receptor alpha; PS: phosphatidylserine; PUFA: polyunsaturated fatty acids; REM: remission patients; REL: relapse patients; ROC: receiver operative characteristic; RRMS: relapsing-remitting multiple sclerosis; RT: retention time; SM: sphingomyelin; SPE: solid phase extraction; XIC: extracted-ion chromatograms.

1. Introduction

Multiple sclerosis is a chronic disease characterized by neurodegeneration, demyelination and (neuro)inflammation, resulting in severe neurological impact and disability in young adults [1]. This pathology is responsible for a progressive disability where the acute phases are the most debilitating for the patients. It affects approximately 2.3 million people worldwide, mostly women [2].

Four disease courses are considered for this disease, classified according with clinical signs and symptoms. These courses are clinically isolated syndrome, relapsing-remitting multiple sclerosis (RRMS), secondary progressive multiple sclerosis and primary progressive multiple sclerosis, of which RRMS is the most common [3,4]. The diagnosis of multiple sclerosis is based on clinical parameters and imaging, but it is a long and often delayed task, preventing early initiation of treatment [5]. Much effort has been made to overcome this drawback, but the early diagnosis of multiple sclerosis remains a difficult task and definitive diagnostic tests are not available. Moreover, the monitoring of disease progression and the efficacy of therapeutic approaches are also based on clinical parameters and lack specific markers or tests to predict or early detect a period of remission [6]. Thus, it is difficult if not impossible to apply early therapeutic or preventive strategies to prevent worsening of symptoms and periods of relapse. Thus, there is a need to find new reliable biomarkers not only to help and improve the diagnosis of multiple sclerosis but also for more accurate monitoring of disease progression [7].

The lack of biomarkers is mainly due to the heterogeneous pathophysiology of this disease which is not fully understood. Multiple sclerosis is a demyelinating disease in which the myelin sheath around the nerves is destroyed [8]. Myelin has a high lipid content, mainly composed of phosphatidylethanolamine, glucosyl-ceramides, phosphatidylcholine, sphingomyelin, ceramides and sulfatides. Changes in its lipid composition may be associated with impaired myelin function [9]. Therefore, lipids would be promising candidates to be useful biomarkers of this disease

[10,11]. Also, lipids are key players in the regulation of inflammatory responses and can modulate activated immune cells in autoimmune diseases [12].

Changes in lipid metabolism and lipid profile have been reported in a few studies of multiple sclerosis, and it has been suggested to play a fundamental role in the pathogenesis and severity of this disease [13,14]. Although most studies have focused on the variation in fatty acid metabolism [6]. The arachidonic acid metabolic pathway has been reported to be overactivated in the central nervous system of patients with multiple sclerosis [15]. Prostaglandins and hydroxyeicosatetraenoic acids were elevated in the cerebrospinal fluid of patients with multiple sclerosis due to overactivation of arachidonic acid metabolism and neuroinflammation[16]. Deficiency of polyunsaturated fatty acids (PUFAs) and increased short-chain FA have also been reported in other studies (as recently reviewed in [6]). Omega-3 lipids, which have a protective role by preserving the blood-brain barrier, are significantly reduced in the serum of patients with multiple sclerosis [17,18].

Regarding phospholipids (PL), lyso-phosphatidylcholines are reduced in plasma [19]. Ceramides (Cer), well-known signalling molecules associated with mitochondrial dysfunction and cell apoptosis, are significantly increased in the plasma and cerebrospinal fluid of patients with multiple sclerosis [20,21]. The lipid peroxidation products of 4-hydroxynonenal, isoprostanes, malondialdehyde and cholesteryl ester hydroperoxides have been found at increased concentrations in plasma and serum of multiple sclerosis [6]. Despite studies showing a positive correlation of lipids in this disease, no study has looked for an alteration in serum PL in this pathology.

Analysis of lipid variation at the molecular level using high-throughput lipidomic techniques provides an understanding of the contribution of lipids to disease development and its molecular mechanisms, which could be useful and have a purpose for the study of several chronic diseases in clinical lipidomics [22,23].

In the present study, we sought to make a comprehensive assessment of the variation in the serum phospholipid profile of patients with multiple sclerosis compared to control patients, using

an untargeted lipidomics approach. It also aimed to assess the differences in lipid profile between disease status (relapse and remission).

2. Materials and methods

2.1 Reagents

To perform the PL separation of the samples by solid-phase extraction, acetonitrile (ACN) was acquired from Fisher Scientific (Leicestershire, UK) and formic acid and ammonium hydroxide were obtained from Sigma-Aldrich Chemical Co. (St. Louis, MO, USA). To quantify the PL in each sample, dichloromethane was purchased from Fisher Scientific, 70% perchloric acid was obtained from Chem-Lab NV (Zedelgem, Belgium), $NaH_2PO_4 \cdot 2H_2O$ was purchased from Riedell-de Haën (Seelze, Germany), ammonium molybdate ($NaMoO_4 \cdot H_2O$) was acquired from Panreac (Barcelona, Spain) and the L(+)-ascorbic acid from VWR Chemicals (Leuven, Belgium). Internal standards of PL 1,2-dimyristoyl-*sn*-glycero-3-phosphocholine (dMPC, PC 14:0/14:0), 1,2-dimyristoyl-*sn*-glycero-3-phosphoethanolamine (dMPE, PE 14:0/14:0), 1,2-dimyristoyl-*sn*-glycero-3-phospho-(10-rac-)glycerol (dMPG, PG 14:0/14:0), 1,2-dimyristoyl-*sn*-glycero-3-phospho-L-serine (dMPS, PS 14:0/14:0), tetramyristoylcardiolipin (TMCL, CL 14:0/14:0/14:0/14:0), 1,2-dipalmitoyl-*sn*-glycero-3-phosphatidylinositol (dPPI, PI 16:0/16:0), N-heptadecanoyl-D-*erythro*-sphingosylphosphorylcholine (SM d18:1/17:0), 1-nonadecanoyl-2-hydroxy-*sn*-glycero-3-phosphocholine (LPC 19:0) and 1,2-dimyristoyl-*sn*-glycero-3-phosphate (dMPA, PA 14:0/14:0) for HILIC-MS analysis were obtained from Avanti® Polar Lipids, Inc (Alabaster, AI, EUA). The solvents for LC-MS were ACN, methanol (Fisher Scientific), Milli-Q water and ammonium acetate (Sigma-Aldrich). Dichloromethane was also purchased from Fisher Scientific. All solvents were of high-performance liquid chromatography (HPLC) grade and were used without any additional purification. Milli-Q water was used for all experiments, filtered through a 0.22mm filter and obtained using a Milli-Q Millipore system (Synergy®, Millipore Corporation, Billerica, MA, USA).

2.2 Serum samples

Serum samples from patients with multiple sclerosis and healthy controls were provided by Centro Hospitalar Cova da Beira (CHCB). Participating patients (n=24) were diagnosed with RRMS and were followed up at CHCB before sample collection for this study. The diagnosis was based on clinical, MRI, and biochemical criteria, according to the 2010 MacDonald criteria [24]. Exclusion criteria were active infections, local or systemic diseases that affect the immune system, pregnancy, and corticosteroids or other treatments for multiple sclerosis in addition to IFN-β. To allow participation in this study, all healthy control volunteers (HC) (n=30) were guaranteed to be healthy, showing no signs of active infection, autoimmune disease, and treatment with immunomodulatory drugs. HC samples were age- and gender-matched. The study protocol was approved by the CHCB`s Ethics Committee. Summary information on patients with multiple sclerosis and healthy controls is shown in Table 1. After collection, serum samples were stored at −80 °C until further study of the lipid profile.

Table 1. Demographic and clinical characteristics of patients with multiple sclerosis (RRMS) and healthy controls (HC).

	Remission RRMS (n=17)	Relapse RRMS (n=7)	HC (n=30)
Age (years)*	46.5 ± 12.3	40.9 ± 14.7	49.5 ± 10.1
Sex (% women)	94.1 %	71.4 %	76.7%
EDSS-score*	1.5 ± 0.8	3.0 ± 1.4	-
Disease duration (years)*	12.2 ± 7.2	4.3 ± 4.0	-

*Values represent the mean ± standard deviation.

2.3 Phospholipid extraction and phosphorus measurement

Solid-phase extraction (SPE) was used to separate PL from serum samples as previously described by Anjos *et al* [25] with modifications. The SPE procedure required three eluents prepared before the extraction of PL. Eluent 1 consisted of ACN with 1% formic acid. Eluent 2 was

pure ACN. Eluent 3 was ACN with 5% ammonium hydroxide. After the preparation of the mobile phases, a volume of 100 µL of serum from each sample was mixed with 900 µL of eluent 1 in a Pyrex tube. Each tube was vortexed for 30 seconds, then centrifuged at 2000 rpm for 5 minutes for protein precipitation. The resulting supernatant from each tube was transferred to a Hybrid SPE-PL column (HybridSPE® - Phospholipid 30 mg, SUPELCO, Sigma-Aldrich, Bellefonte, PA) that was already placed in a vacuum *Visiprep SPE Vacuum Manifold* (SUPELCO) system and previously conditioned with 1 mL of ACN. After elution of almost all the supernatant, the columns were washed with 1 mL of eluent 2 and with 1 mL of eluent 1. At this stage, the collection tubes were replaced by new ones and the PL retained on the Hybrid SPE-PL columns were eluted with two consecutive 1 mL aliquots of eluent 3. The flow-through was collected and dried under a stream of nitrogen. The samples were dissolved in 400 µL of dichloromethane and transferred individually to a HAMILTON glass syringe. All samples were filtered with a Millex® - LH 0,45 µm filter (low protein binding hydrophilic LCR Membrane for clarification of aqueous and organic solutions). The filtered samples were collected in vials and dried under a stream of nitrogen.

2.4 Phospholipid quantification by phosphorous measurement

The quantification of the total PL recovered after extraction was carried out according to the method of Bartlett & Lewis [26]. The detailed experimental procedures have been previously described by Anjos *et al* [25]. The PL extracts were dissolved in 100 µL of dichloromethane, and a volume of 10 µL was transferred, in duplicate, to a glass tube, previously washed with 5% nitric acid. The solvent was dried under a stream of nitrogen and a volume of 125 µL of 70 % perchloric acid was added to each tube. The samples were incubated in a heat block (Stuart, U.K.) for 1h at 180 °C. After cooling to room temperature, a volume of 825 µL of Milli-Q water, 125 µL of 2.5% ammonium molybdate (2.5 g/ 100 mL of Milli-Q water), and 125 µL of 10% ascorbic acid (0.1 g/1 mL of Milli-Q water) were added to each sample, with a vortex mixing between each addition. The samples were then incubated in a 100 °C water bath for 10 min. Then the samples were immediately cooled in a cold-water bath. Phosphate standards of 0.1 to 2 µg of phosphorus (P)

were prepared from sodium dihydrogen phosphate dihydrate ($NaH_2PO_4 \cdot 2H_2O$, 100 μg/mL of P). The standards underwent the same experimental procedure as the samples without the heat block step. Absorbance was measured at 797 nm in a Multiskan GO 1.00.38 Microplate Spectrophotometer (Thermo Scientific, Hudson, NH, USA) controlled by SkanIT software version 3.2 (Thermo Scientific™). The amount of P present in each sample was calculated by linear regression. For each lipid extract, the amount of total PL was calculated by multiplying the amount of phosphorus by 25.

2.5 Lipid extract analysis by Hydrophilic interaction liquid chromatography-mass spectrometry (HILIC-MS)

2.5.1 Sample preparation

The PL extracts obtained from serum samples were resuspended in dichloromethane to have a PL concentration of 1 μg PL/μL. Subsequently, in a vial with a micro-insert, 5 μL of each sample, 4 μL of a mixture of internal standards and 91 μL of the initial chromatographic phase were added. The internal standard mixture contained 0.02 μg of phosphatidylcholine (PC, 14:0/14:0), 0.02 μg of phosphatidylethanolamine (PE, 14:0/14:0), 0.012 μg of phosphatidylglycerol (PG, 14:0/14:0), 0.08 μg of phosphatidylinositol (PI, 16:0/16:0), 0.04 μg of phosphatidylserine (PS, 14:0/14:0), 0.08 μg of phosphatidic acid (PA, 14:0/14:0), 0.02 μg of lyso-PC (LPC, 19:0), 0.02 μg of sphingomyelin (SM, d18:1/17:0) and 0.08 μg of cardiolipin (CL, 14:0/14:0/14:0/14:0). The initial chromatographic phase consisted of two mobile phases at a proportion of 10% of eluent A (50% acetonitrile, 25% methanol, 25% water and 2.5 mM ammonium acetate) and 90% of eluent B (60% acetonitrile, 40% methanol and 2.5 mM ammonium acetate).

2.5.2 Data and statistical analysis

The PL were separated by HILIC, according to the polarity of the moiety group, using an Ascentis Si HPLC Pore column (100 mm x 1 mm; 3 μm, Sigma-Aldrich) inserted into an HPLC system (Ultimate 3000 Dionex, Thermo Fisher Scientific, Bremen, Germany) with an autosampler

coupled online to a Q-Exactive™ Hybrid Quadrupole-Orbitrap™ Mass Spectrometer (Thermo Fisher Scientific, Bremen, Germany).

A volume of 5 μL of each sample mixture was injected into the HPLC column, at a flow rate of 50 μL/min. The temperature of the column oven was maintained at 35 °C. Elution started with 10% of mobile phase A, which was held isocratically for 2 minutes, followed by a linear increase to 90% of mobile phase A within 13 minutes and maintained for 2 minutes. After that, conditions returned to the initial settings in 13 minutes (3 min to decrease to 10% of phase A and a re-equilibration period of 10 min prior next injection). The Q-Exactive™ orbitrap mass spectrometer with a heated electrospray ionization source was operated using a positive/negative switching toggles between positive (electrospray voltage of 3.0 kV) and negative modes (electrospray voltage of −2.7 kV). The sheath gas flow was 15 U, auxiliary gas was 5 U, the capillary temperature was 250 °C, the S-lenses RF was 50 U and the probe`s temperature was 130 °C. Full scans MS spectra were acquired both in positive and negative ionisation modes in an *m/z* range of 400-1600, with a resolution of 70.000, automatic gain control (AGC) target of $1x10^6$ and maximum injection time of 100 ms. For tandem MS (MS/MS) experiments, a top-10 data-dependent method was used. The top 10 most abundant precursor ions in full MS were selected to be fragmented in the collision cell HCD. A stepped normalized collision energy™ scheme was used and ranged between 20, 25 and 30 eV. MS/MS spectra obtained were those combining the information obtained with the three collision energies. The MS/MS spectra were obtained with a resolution of 17,500; AGC target of $1x10^5$; an isolation window of 1 *m/z*; scan range of 200-2000 *m/z*; and maximum injection time of 50 ms. The cycles consisted of one full scan mass spectrum and ten data-dependent MS/MS scans, which were repeated continuously throughout the experiments, with the dynamic exclusion of 60 s and intensity threshold of $1x10^4$. Data acquisition was carried out using the Xcalibur data system (V3.3, Thermo Fisher Scientific, USA).

LC-MS data were processed and integrated using the MZmine v2.42 software [27]. This software enabled filtering and smoothing, PL peak detection, PL peak alignment and integration,

and PL assignment and identification against an in-house database, which contains information on the exact mass and retention time (RT) for each PL molecular species. The identification of the PL species was performed as described previously [25,28]. Briefly, to correctly identify the PL species, during the processing of raw data by MZmine, all peaks of raw intensity less than $1x10^4$ and error greater than 5 ppm were excluded. The assignment of each PL species was confirmed by analysis and interpretation of the MS/MS spectra. PC, LPC and SM were analysed in the LC-MS spectra in the positive ion mode, as $[M+H]^+$ ions. The presence of the fragment ion at *m/z* 184, corresponding to the phosphocholine polar head group, in the MS/MS of $[M+H]^+$ ions allows identifying PL molecular species belonging to the PC, LPC and SM classes, which were further differentiated by the characteristic retention times. PC, LPC and SM were also analysed in the LC-MS spectra in the negative ion mode, as acetate adducts ($[M+CH_3COO]^-$ ions). MS/MS spectra of $[M+CH_3COO]^-$ ions of these three PL classes should display the typical fragment ion at *m/z* 168 (phosphocholine polar head group minus a methyl moiety). Carboxylate anions of fatty acyl chains can also be seen for PC and LPC. PE and LPE classes were analysed both in positive ($[M+H]^+$ ions) and negative ion modes ($[M-H]^-$ ions). The neutral loss of 141 Da (phosphoethanolamine polar head group) can be observed in the MS/MS acquired in the positive mode, while the fragment ion at *m/z* 140 (phosphoethanolamine polar head group) and the carboxylate anions of fatty acyl chains can be found in MS/MS data from negative ion mode. For structural identification of PC, LPC, SM, PE and LPE, the MS/MS data was analysed in positive and negative ion modes, however, for quantification purposes, only LC-MS positive ion mode data was used. PI and PG species together with the lyso forms of PI (LPI) and PG (LPG) were analysed in negative ion mode, as $[M-H]^-$ ions. These species were identified based only on the RT and exact mass measurements, no MS/MS spectrum was found. An example of the MS/MS fragmentation patterns of each PL classes analysed in the present study is available in the supplementary material.

Relative quantification was performed by exporting the peak area values to a computer spreadsheet. For normalization of the data, the peak areas of the extracted ion chromatograms

(XIC) of the PL precursors of each class were divided for the peak area of the internal standards selected for the class.

The data sets composed of the XIC areas obtained by the HILIC-MS analysis were normalized to the internal standard, generalized log2, normalized with EigenMS [29], autoscaled and analysed statistically. Missing values were replaced with half of the minimum positive values detected in the data set. Principal component analysis (PCA) was performed using the R libraries FactoMineR [30] and factoextra [31], and the ellipses were drawn assuming a multivariate normal distribution and a level of 0.95. Univariate statistical analysis was performed using the Wilcoxon or Kruskal−Wallis test following a post hoc Dunn test. A *p*-value < 0.05 was considered an indicator of statistical significance. Heatmaps were created using the R package pheatmap using "Euclidean" as the clustering distance and "ward.D" as the clustering method [32]. Univariate and multivariate statistical analyses were performed using R version 3.5.1 in Rstudio version 1.1.4. All graphics and boxplots were created using the R package ggplot2 [33]. Other R packages used for data management and graphics included plyr [32],

dplyr [34] and tidyr [35]. The areas under curve (AUC) of Receiver operative characteristic (ROC) curves were used to determine the diagnostic effectiveness of important phospholipids using the R packages Caret [36], using a Random Forest model with the default parameters, and pROC [37].

3. Results

3.1 Characterization of the serum samples

To assess the changes in the PL profile associated with multiple sclerosis, we analysed the serum of 24 patients diagnosed with multiple sclerosis (from now on referred to as MSs) and 30 healthy controls samples (HC), as summarized in Table 1. All patients and controls were adults aged 20 to 60 years. A total of 94.1% and 71.4% of the patients in remission (MSs_Rem) and relapse (MSs_Rel), respectively, were female.

3.2 Identification of the serum phospholipid profile of patients with MSs and HC

The PL profile of MSs and HC serum was analysed by high-resolution HILIC-MS and MS/MS platform. This lipidomic analysis allowed to identify 161 different PL species (molecular ions) belonging to 9 different classes, namely phosphatidylcholine (PC) comprising diacyl, alkyl-acyl and alkenyl-acyl species, lyso PC (LPC), phosphatidylethanolamine (PE) including diacyl, alkyl-acyl and alkenyl-acyl species, lyso PE (LPE), phosphatidylglycerol (PG), lyso PG (LPG), phosphatidylinositol (PI), lyso PI (LPI) and sphingomyelin (SM) (Supplementary Table S1). PC, LPC, PE, LPE and SM species were identified by analysis of exact mass, retention time and MS/MS spectra, while PG, LPG, PI and LPI species were identified by exact mass and retention time. Statistical analysis, including multivariate and univariate statistical analysis grouped the data

as follows: 1) comparing HC with MSs (healthy *vs* overall disease) and 2) comparing HC with MSs_Rem and MSs_Rel patients.

3.2.1 Comparison of serum phospholipidome from HC versus patients with MSs (health *vs* disease)

The differences between the PL profile of HC (30 controls) and patients with MSs (24 patients), regardless the disease state (remission or relapse), were assessed using multivariate statistical analysis. Data from LC-MS analysis were auto-scaled and then subjected to principal component analysis (PCA) to show the clustering trends of the two experimental groups. The PCA plot showed that the two groups were separated in two different clusters, in a two-dimensional score plot that represented the analysis describing 31.3% of the total variance, including dimension 1 (24%) and dimension 2 (7.3%), with major discrimination in dimension 1 (Figure 1). HC samples were scattered on the right region of the PCA plot while MSs samples were scattered on the left region.

Considering the variables that contributed the most to group discrimination, 16 PL molecular species were identified that showed the most significant discriminating power between conditions using variable importance in projection (VIP) (Supplementary Figure S4). Eight of these PL species with higher discriminating potential were ether-linked (akyl-acyl and alkenyl-acyl), PC (5 species) and PE (3 species), which are generally decreased in MSs.

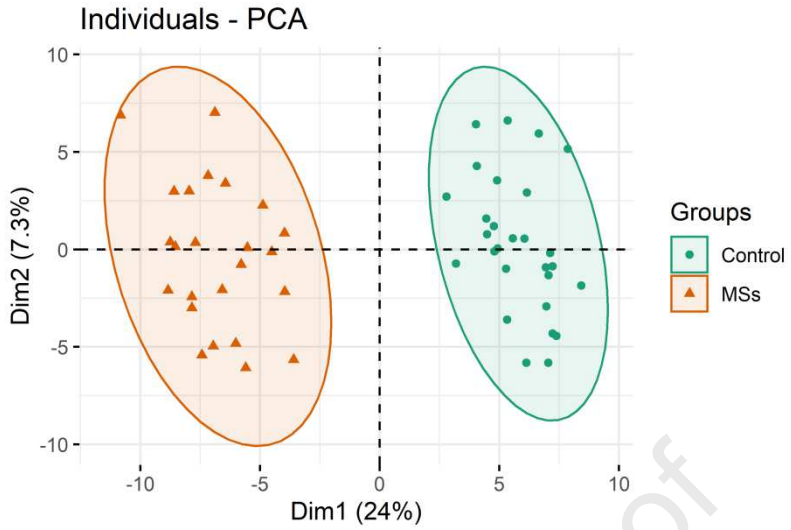

Figure 1. Principal component analysis (PCA) in a two-dimensional score scatter plot of PL profiles from serum from healthy control (Control) and disease (MSs) groups.

Also, a univariate analysis of the HILIC-MS data of the two conditions was performed (Supplementary Table S2), and the Wilcoxon test showed that the 16 major contributors with the lowest *q*-value ($q<0.05$) were selected (Figure 2) corresponding to 7 PC, 3 ether-linked PC, 3 ether-linked PE, and 3 LPE species, all with statistically significant lower levels in MSs. We predicted the test dataset using a trained model and found that the random forest predicts with an accuracy of 100%. Next, we have performed a Receiver operative characteristic (ROC) analysis to further characterize the predictive value of these top 5 PL independently (Supplementary Figure S5). We found that all 5 PL had an area under the curve (AUC) >0.96.

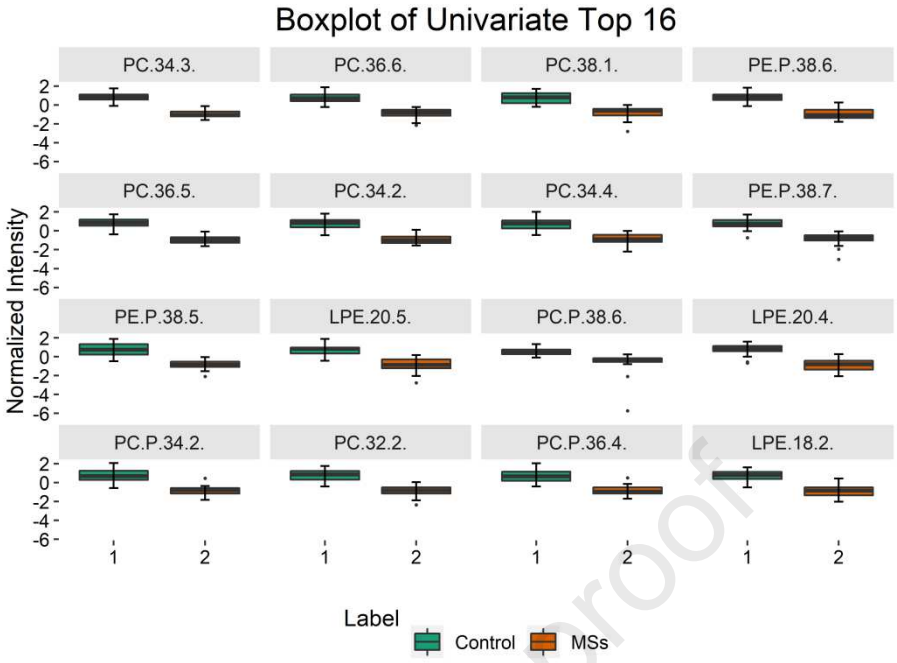

Figure 2. Box plots of the 16 most discriminating PL species with the lowest q-values obtained from a univariate analysis of HC (1) and MSs patients (2) using the Wilcoxon test. $q < 0.05$ for all comparisons.

Additionally, we carried out a hierarchical clustering analysis (HCA) on the phospholipid data sets from the two conditions (Figure 3). The results were used to create a heatmap of the top 25 PL species with the lowest q-values in the Wilcoxon test, and a dendrogram with a two-dimensional hierarchical clustering of the functional state and variables that reflect the most important native PL species contributing to differentiate MSs disease from HC. The resulting HCA dendrogram (Figure 3) showed a noticeable separation of the two data in the first dimension (upper hierarchical dendrogram) where samples are clustered independently into two groups, control and disease (MSs). Moreover, the clustering of individual PL species also shows two principal clusters: the first group includes a single PL specie, PE(40:10), which is more abundant in MSs, while the second group had 24 different PL species which are less abundant in MSs than HC, and included 11 plasmalogens species, namely 6 PE plasmalogens, 5 PC plasmalogens, 8 PC species (with 7 PC bearing PUFA), 3 LPE with PUFA, 1 PE and 1 PG species.

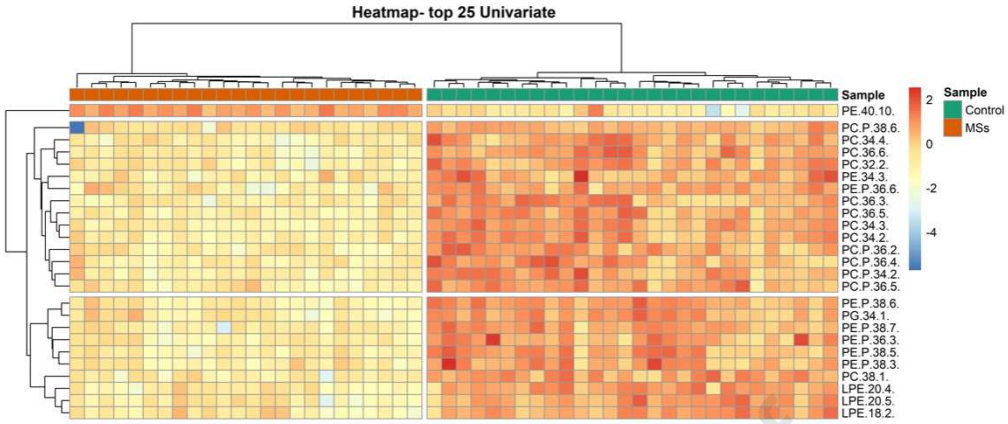

Figure 3. Two-dimensional hierarchical clustering heatmap of the 25 most discriminating PL molecular species of Control and MSs groups. Relative abundance levels are shown on the red-yellow-blue scale, with the numbers indicating the fold difference from the overall mean. The red colour of the tile indicates high abundance and blue indicates low abundance. Null values were displayed in yellow. The clustering of the control and disease groups is represented by the dendrogram at the top. The clustering of individual PL molecular species is represented by the dendrogram on the left.

3.2.2 Comparison of serum phospholipidome from HC versus patients with MSs_Rem and MSs_Rel

The PL profile was compared considering the disease status. Thus, the MSs PL profile of the serum from the two groups, MSs_Rem (n=17) and MSs_Rel (n=7), were compared to HC. Multivariate analysis of the datasets was performed and the PCA plot generated showed that, in a two-dimensional score plot, the HC group separates from the two MSs groups (Figure 4). The PCA plot also showed the separation of the two conditions, MSs_Rem and MSs_Rel, although some overlapping of the 95% confidence ellipse was observed. The PCA score plot described 32.7.% of the total variance, including dimension 1 (24.8%) and dimension 2 (7.9%), where dimension 1 was the major discriminant. The HC samples were scattered in the right region of the plot while the

MSs_Rem and MSs_Rel samples were scattered on the left region of the plot. The 16 PL molecular species that showed the most significant discriminating power between conditions in PCA analysis (Supplementary Figure S6), using VIP scores, included 7 PC (2 diacyl PC plus 5 alkyl-acyl PC), 4 PE (2 diacyl PE and 2 PE plasmalogens), 2 PG, 1 PI, 1 LPE and 1 LPG specie. Boxplots, which report the normalized intensities of the 16 PL species, show the PL species with higher discriminating potential between MSs groups, such as PE (P-34:5), PE (30:2) and LPG14:0 species which were found to have lower levels in MSs_Rel than in HC and MSs_Rem.

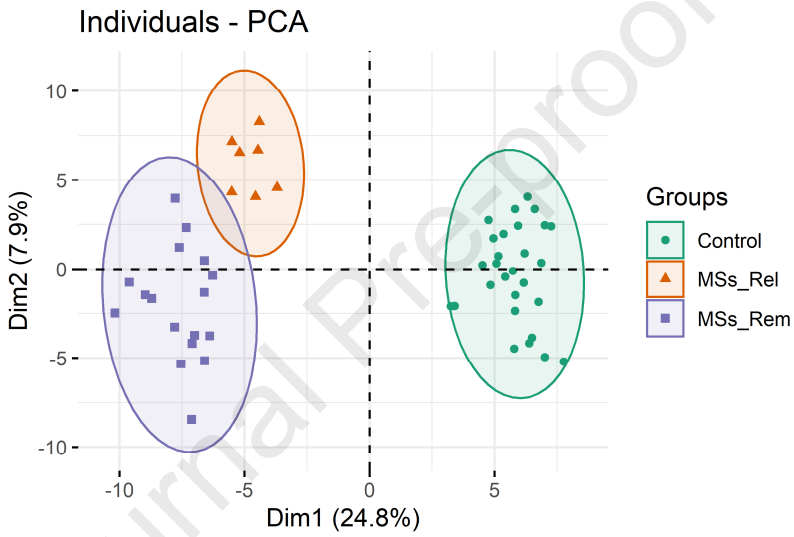

Figure 4. PCA of the serum phospholipidome from control, MSs_Rel and MSs_Rem. PCA in a two-dimensional score scatter plot of PL profiles obtained in both positive and negative modes from healthy control (Control), MSs_Rel and MSs_Rem groups.

Also, a univariate analysis (Kruskal−Wallis test followed by Dunn's multiple comparison post-hoc test) was performed on the HILIC-MS data, to test for significant differences between the three conditions (Supplementary Table S3). The main 16 contributors from the Kruskal−Wallis test with the lowest *q*-value (with q<0.05) were selected (Figure 5) and correspond to 7 PC, 2 ether-linked PC, 5 ether-linked PE, and 2 LPE species, all with statistically significantly higher levels in control samples. Dunn's test of multiple comparisons revealed that 16 species were significantly

different between HC and MSs_REM, 15 between HC and MSs_REL, and 1 (PC 38:1) between MSs_REL and MSs_REM.

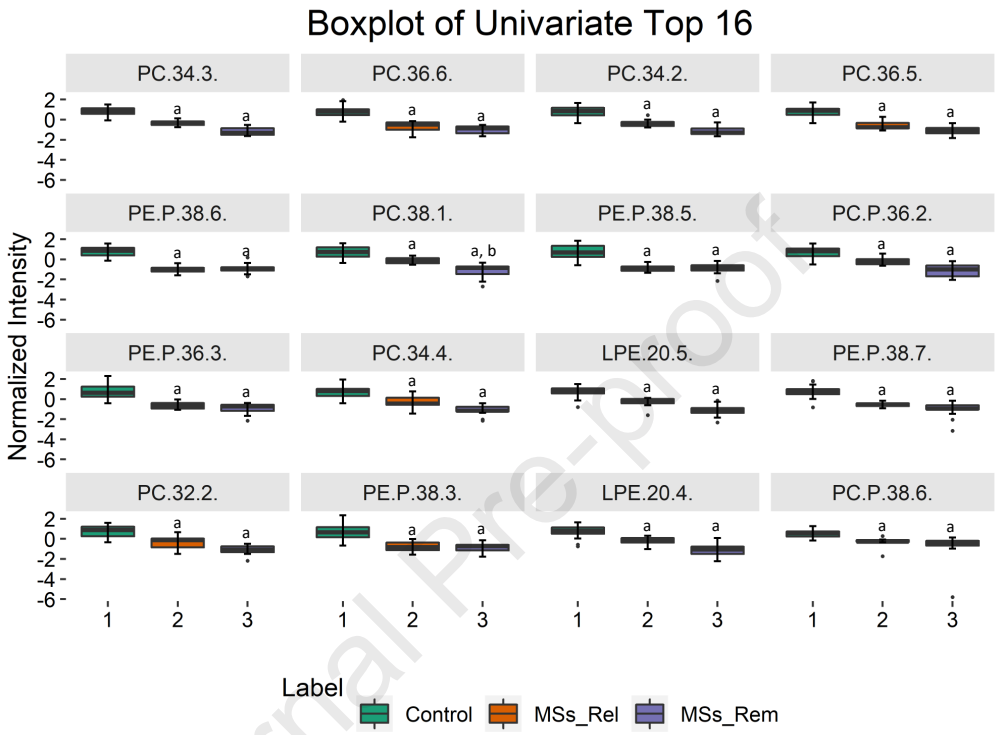

Figure 5. Box plots of PL molecular species with the lowest 16 q-values of the Kruskal-Wallis test followed by the Dunn multiple comparison tests of Control, MSs_Rel and MSs_Rem. $q < 0.05$ was considered statistically significant: a, control vs MSs_Rem and control versus MSs_Rel; b, MSs_Rel versus MSs_Rem.

The results of the Kruskal-Wallis test were also used to create a heatmap of the 25 PL species with the lowest q-values. The dendrogram with two-dimensional hierarchical clustering of disease status and variables (Figure 6) shows the most important native PL species contributing to differentiate MSs-Rel and MSs-Rem from HC samples. It is possible to observe that in the first dimension, in the top hierarchical dendrogram, the samples are clustered independently into two groups, control versus disease, and it was not possible to achieve complete discrimination between the two statuses of disease. The clustering of the individual PL species allowed for the

identification of two principal clusters: the first which included 6 ether-linked PE that is more abundant in the HC group and less abundant in the disease groups, while the second contains different PL species which are also more abundant in the HC group and the MSs-Rel, but with low abundance in MSs-Rem, including 4 PC plasmalogens, 8 PC(including 6 PC bearing PUFA) and 3 LPE species and 1 LPC.

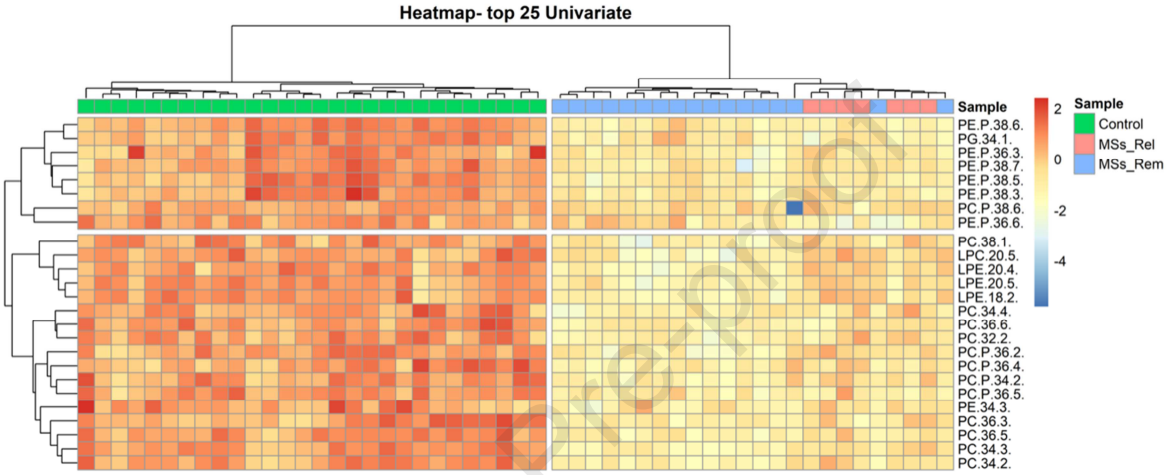

Figure 6. Two-dimensional hierarchical clustering heat map of the 25 most discriminating PL molecular species of the control, MSs_Rel and MSs_Rem groups. Relative abundance levels are shown on the red-yellow-blue scale, with the numbers indicating the fold difference from the overall mean. The red colour of the tile indicates high abundance and blue indicates low abundance. Null values were displayed in yellow. The clustering of the HC, MSs_Rel and MSs_Rem groups is represented by the dendrogram at the top. The clustering of individual PL molecular species is represented by the dendrogram on the left.

Univariate analysis (Figure 2 and Figure 5) indicates that the 16 PL molecular species that most significantly contribute to discriminating HC from MSs and HC from patients with MSs_Rem and MSs_Rel mainly include PC and PE species, bearing PUFA, and PC and PE alkyl-acyl species, and some lyso PL. There was variation in 13 PL molecular species revealing the lowest abundance of PC(34:3); PC(36:6); PC(38:1); PE(P-38:6); PC(36:5); PC(34:2); PC(34:4); PE(P-38:7); PE(P-

38:5)/PE(O-38:6); LPE(20:5); PC(P-38:6); LPE(20:4) and PC(32:2) in MSs (overall disease) and MSs_Rem and MSs_Rel. ROC analysis (supplementary figure S5) have shown, that the five variables with the lowest p-value distinctive had very high AUC value (>0.96) two had a AUC > 0.99 (PC(34:3) and PC(36:6)), showing a potential high diagnostic performance of multiple sclerosis. The boxplots in Figure 2, which compared HC with MSs, also showed that PC(P-34:2)/PC(O-34:3); PC(P-36:4)/PC(O-36:5) and LPE(18:2) were significantly downregulated in MSs and contributed to differentiate the two groups. In the second analysis (Figure 5), PC(P-36:2)/PC(O-36:3); PE(P-36:3)/PE(O-36:4) and PE(P-38:3)/PE(O-38:4) were also significantly decreased in the MSs_Rem and MSs_Rel groups. The lower levels of PC(34:3); PC(34:2); PC(36:5); PC(38:1); PC(P-36:2)/PC(O-36:3); PC(34:4); LPE(20:5); PC(32:2) and LPE(20:4) in the MSs_Rem group show a deeper alteration in lipid metabolism. The result of the hierarchical cluster analysis represented by a heatmap (Figures 3 and 6) also confirms that PC and PE are the PL classes that contribute the most to differentiate all the groups.

4. Discussion

Lipids have important biological functions with critical roles in inflammatory and immune processes and have been correlated with the pathophysiology of many diseases, including autoimmune diseases such as MSs [6]. They have been shown to contribute to the pathogenesis and severity of MSs. MSs is characterized by demyelination and myelin is mainly composed of lipids, but their role in MSs is scarcely addressed [10]. In this study, a phospholipidomic profiling of serum samples from patients with MSs was carried out, aiming to elucidate the adaptations of the PL profile concerning the health status, and associated with the different statuses of this disease. Lipidomics data were analyzed by multivariate principal component analysis (PCA) as well as univariate and hierarchical cluster analysis (HCA) for visualization and interpretation of results. Of all the patients included in this study, a total of 94.1% of MSs_Rem patients and 71.4% of

MSs_Rel patients were female, which is in agreement with the epidemiological evidence indicating that MSs is three times more prevalent in women [38].

Initially, a comparison between healthy controls and patients with the disease (HC vs MSs) was performed to assess the differences between health and disease. Analysis of the PCA score plot (Figure 1) indicated that the lipidome of the two conditions differ from each other, which means that the serum PL profile of MSs is different from HC. Then the lipid profile was also compared taking into account the status of the disease. RRMS is characterized by periods of relapse and remission that affect the patient's daily life. During periods of relapse, the (neuro)inflammatory conditions worsen, so it is expected to observe major or dissimilar changes in the lipid profile. The analysis of PCA scores scatter plot (Figure 4) revealed that HC differed from MSs, however, the MSs_Rem and MSs_Rel 95% confidence ellipses partially intercept and as such are not fully discriminated. This means that while considering that in remission there are fewer (if any) symptoms, there is also a modulation of the lipid profile which is different from typical health conditions. Even in the absence of symptoms, the lipid profile does not return to the level of healthy status and the significance of this imbalance should be carefully assessed.

In this work, patients with MSs had a lower abundance of plasmalogens PC and PE species, compared to controls, and differences were mainly observed in PC and PE species with PUFA. PC is the most abundant class of PL in cell membranes and plasma [39]. In our models, few PC species discriminated HC from MSs and HC from MSs_Rem and MSs_Rel. Different PC species have contributed to this differentiation such as plasmalogens PC(P-38:6); PC(P-36:2)/PC(O-36:3); PC(P-36:4)/PC(O-36:5); PC(P-34:2)/PC(O-34:3); PC(P-36:5) and the diacyl species PC(34:4); PC(36:6); PC(32:2); PC(36:3); PC(36:5); PC(34:3); PC(34:2) and PC(38:1). However, only PC(38:1) was statistically different between MSs_Rel and MSs_Rem, being lower in MSs_Rem (Figure 5). PC(38:1) was identified as PC(18:1/20:0), thus bearing an oleic acid (FA 18:1). Trépanier et al reported a significant reduction in oleic acid in post-mortem brain tissue from mouse models with induced demyelination and from patients with MSs [40]. In our study, comparing HC to MSs groups, we also found significantly lower levels of the molecular species

PC(34:2), PC(36:3), and PC(38:1), all of which contained oleic acid in their composition. Cicalini *et al* also found a markedly decreased PC(38:1) in tears from patients with MSs [41]. The decrease in PL species may be due to a decrease in oleic acid biosynthesis which may result from the dysregulation of different pathways, such as i): reduced formation and levels of 18:1 precursors, namely palmitate (C16:0), stearate (C18:0) or palmitoleate (C16:1); ii) this may be the result of downregulation of desaturases, as Δ9-desaturase, which converts FA 18:0 into FA 18:1 n-9 and FA 16:0 into FA 16:1 n-9; or iii) it may ultimately derive from the downregulation of ELOVL6 elongase which converts FA 16:0 into FA 18:0 (Supplementary Figure S7).

PE is the second most abundant class of PL in cells and is the major class of PL in myelin sheaths. The results gathered in the present work showed that the PE species contributed to differentiate HC from MSs and HC from MSs_Rel and MSs_Rem. These species were PE(34:3); PE(P-36:6); PE(P-38:6); PE(P-38:7); PE(P-36:3)/PE(O-36:4); PE(P-38:5)/PE(O-38:6); PE(P-38:3)/PE(O-38:4), generally lower in disease. Another feature noted when comparing MSs phospholipidome (overall disease) with HC, was the significantly higher concentrations of PE(40:10) in MSs. The majority of PC and PE species that showed variation were esterified to PUFA and were decreased in MSs. The significant reduction in serum PE and PC species in MSs has also been reported by Villoslada et al[42].

PE may have a role in the immune response by modulating CD300 receptor in chronic inflammatory diseases and are also known to participate in autoimmune diseases. However, the exact function of the receptors of this family is unclear and may upregulate or downregulate immune responses [43]. PC is fundamental in proliferative growth and programmed cell death [44]. Therefore, these alterations in phospholipidome may be correlated with increased chronic activation of the immune system in patients with MSs, in which PL have important functions [45]. In addition, we have found among the PC and PE species several ether-linked species, namely the PC and PE plasmalogens. These species had significantly lower levels in MSs, MSs_Rel and MSs_Rem, compared to controls. Plasmalogens are considered to be important endogenous antioxidants, playing a key role in cellular antioxidant defence, so their reduction in disease

conditions may be an indicator of an increased oxidative environment in MSs [46,47]. Plasmalogens have also been recognised as important antioxidants in myelin [46]. Myelin is highly enriched in PE species, in particular in plasmalogens, and the decrease in PE may be due to damage to the myelin that occurs during demyelination [48,49]. Plasmalogen-deficient mammalian cells are considerably more susceptible to oxidative stress-induced death than high plasmalogen mammalian cells, corroborating the protective role of plasmalogens as antioxidants [46,50,51]. Accordingly, our results of significantly lower abundances of PC and PE plasmalogen species in MSs serum may indicate alterations of the myelin lipid-rich sheaths, making them more vulnerable to oxidative damage, known to be increased in this pathology.

In this work, we found that several PC and PE phospholipids bearing PUFA species had significantly lower abundances in MSs. This decrease could be due to degradation by lipid peroxidation processes that can occur in MSs, in the two groups with different disease status. An increase in oxidative stress has been described in MSs, leading to exacerbation of disease activity and severity [6,52]. The identification of oxidized lipids was not the scope of our work, but oxidized PL has already been found in the plasma of patients with MSs [42,53,54].

The LPE class also contributed to the discrimination of HC and MSs and of HC, MSs_Rem and MSs_Rel, particularly with three species, LPE(20:4); LPE(20:5) and LPE(18:2). These LPE species with PUFA were shown to be significantly reduced in MSs, which correlates well to the results showing that patients with MSs have a FA 18:2, 20:4 and PUFA deficiency in plasma and serum [6]. PUFA are also known to have immunomodulatory effects which are associated with their ability to suppress T cell activation and function [55]. Thus, the reduction in PUFA levels in patients with MSs observed in our work indicates that this may contribute to the activation of T cells in this pathology. MS is mediated by effector T cells, even in remission MSs patients the IL-17 and Th/c17 cells seemed to contribute to perpetuating chronic inflammation [56]. Moreover, the decrease in LPE(20:5) in MSs is noteworthy because LPE(20:5) can arise from degradation of PE(40:10) by phospholipases [57]. In the analysis of control versus MSs, PE(40:10) shows higher abundances in patients with MSs which may indicate altered PLA2 activity in patients with MSs

and decreased LPE(20:5) biosynthesis. For future work, it would be interesting to investigate PLA2 activity. In the HC vs MSs_Rem and MSs_Rel comparison, LPC(20:5) also contributes to differentiate the lipid profile, being downregulated in MSs_Rem and MSs_Rel patients.

Del Boccio *et al* [19], Kurz *et al* [20] and De Oliveira *et al* [58] also analysed MSs plasma and serum samples using LC-MS/MS techniques but these authors only explored alterations on lyso-PL[19], ceramides[20] and other lipid species[58]. To our knowledge, our study is the first to assess phospholipidome changes of several classes of PL using LC-MS/MS.

5. Conclusion

From this study, we can conclude that the pathogenesis of MSs was associated with changes in the lipid profile and that patients with MSs have a significantly different PL profile compared to healthy controls. Our results showed that the phospholipidomic signature of MSs is significantly different from that of healthy controls, in particular for the PE, PC, LPE and ether-linked PE and PC species. Based on the comparison of MSs_Rel and MSs_Rem, our models had less discriminating power, and the species that showed significant differences were mainly PC species, particularly PC(38:1). PC and PE plasmalogens, as well as PC and PE species bearing PUFA, had significantly lower levels in MSs disease and MSs_Rel and MSs_Rem. PE(40:10) and PC(38:1) may be considered as possible serum biomarkers of this disease due to their significant variations in patients with MSs and may be suitable for clinical applications. These results provide new insights on changes in the lipidome profile in MSs and may help improve our understanding of the characteristics of MSs pathogenesis. Clinical lipidomics is one of the best approaches to better understand these disease-induced changes and find suitable biomarkers for personalized MSs medicine.

Acknowledgements

Thanks are due for the financial support to the University of Aveiro and FCT/MCT for the financial support for the CESAM (UIDB/50017/2020+UIDP/50017/2020), QOPNA (FCT UID/QUI/00062/2019), LAQV/REQUIMTE (UIDB/50006/2020) and to RNEM, Portuguese Mass Spectrometry Network (LISBOA-01-0145-FEDER-402-022125) through national funds and, where applicable, co-financed by the FEDER, within the PT2020. Tânia Melo thanks the research contract under the project OMICS 4ALGAE (POCI-01-0145-FEDER-030962).

References

[1] R. Rahmanzadeh, W. Brück, A. Minagar, M.A. Sahraian, Multiple sclerosis pathogenesis: Missing pieces of an old puzzle, Rev. Neurosci. 30 (2019) 67–83.

[2] G.G. Ortiz, F.P. Pacheco-Moisés, O.K. Bitzer-Quintero, A.C. Ramírez-Anguiano, L.J. Flores-Alvarado, V. Ramírez-Ramírez, M.A. Macias-Islas, E.D. Torres-Sánchez, Immunology and oxidative stress in multiple sclerosis: Clinical and basic approach, Clin. Dev. Immunol. 2013 (2013) 1–14.

[3] B.J. Hurwitz, The diagnosis of multiple sclerosis and the clinical subtypes, Ann. Indian Acad. Neurol. 12 (2009) 226–230.

[4] A.J. Thompson, B.L. Banwell, F. Barkhof, W.M. Carroll, T. Coetzee, G. Comi, J. Correale, F. Fazekas, M. Filippi, M.S. Freedman, K. Fujihara, S.L. Galetta, H.P. Hartung, L. Kappos, F.D. Lublin, R.A. Marrie, A.E. Miller, D.H. Miller, X. Montalban, E.M. Mowry, P.S. Sorensen, M. Tintoré, A.L. Traboulsee, M. Trojano, B.M.J. Uitdehaag, S. Vukusic, E. Waubant, B.G. Weinshenker, S.C. Reingold, J.A. Cohen, Diagnosis of multiple sclerosis: 2017 revisions of the McDonald criteria, Lancet Neurol. 17 (2018) 162–173.

[5] C. Tur, A.J. Thompson, Early accurate diagnosis crucial in multiple sclerosis, Practitioner.

259 (2015) 21–27.

[6] H.B. Ferreira, B. Neves, I.M. Guerra, A. Moreira, T. Melo, A. Paiva, M.R. Domingues, An overview of lipidomic analysis on different human matrices of multiple sclerosis, Mult. Scler. Relat. Disord. 44 (2020) 102189.

[7] O. Ciccarelli, A. Thompson, Managing the complexity of multiple sclerosis., Nat. Rev. Neurol. 12 (2016) 70–72.

[8] S. Love, Demyelinating diseases., J Clin Pathol. 59 (2006) 1151–1159.

[9] S. Schmitt, L.C. Castelvetri, M. Simons, Metabolism and functions of lipids in myelin, Biochim. Biophys. Acta - Mol. Cell Biol. Lipids. 1851 (2015) 999–1005. http://dx.doi.org/10.1016/j.bbalip.2014.12.016.

[10] G. Cermenati, N. Mitro, M. Audano, R.C. Melcangi, M. Crestani, E. De Fabiani, D. Caruso, Lipids in the nervous system: From biochemistry and molecular biology to patho-physiology, Biochim. Biophys. Acta - Mol. Cell Biol. Lipids. 1851 (2015) 51–60.

[11] C.E. Hayes, J.M. Ntambi, Multiple sclerosis: Lipids, Lymphocytes and Vitamin D, Immunometabolism. 2 (2020) 1–53.

[12] H.B. Ferreira, A.M. Pereira, T. Melo, A. Paiva, M.R. Domingues, Lipidomics in autoimmune diseases with main focus on systemic lupus erythematosus, J. Pharm. Biomed. Anal. 174 (2019) 386–395.

[13] H. Lassmann, W. Brück, C.F. Lucchinetti, The Immunopathology of Multiple Sclerosis: An Overview., Brain Pathol. 17 (2007) 210–218.

[14] A.P. Corthals, Multiple Sclerosis is Not a Disease of the Immune System., Q. Rev. Biol. 86 (2011) 287–321.

[15] S. Palumbo, Pathogenesis an Progression of Multiple Sclerosis: The Role of Arachidonic

Acid – Mediated Neuroinflammation, in: I. Zagon, P. McLaughlin (Eds.), Mult. Scler. Perspect. Treat. Pathog., Codon Publications, Brisbane, Australia, 2017: pp. 111–123.

[16] N. Mattsson, M. Yaong, L. Rosengren, K. Blennow, J.-E. Månsson, O. Andersen, H. Zetterberg, S. Haghighi, I. Zho, D. Pratico, Elevated cerebrospinal fluid levels of prostaglandin E2 and 15-(S)-hydroxyeicosatetraenoic acid in multiple sclerosis., J. Intern. Med. 265 (2009) 459–464.

[17] S. Bittner, T. Ruck, M.K. Schuhmann, A.M. Herrmann, H.M. ou Maati, N. Bobak, K. Göbel, F. Langhauser, D. Stegner, P. Ehling, M. Borsotto, H.-C. Pape, B. Nieswandt, C. Kleinschnitz, C. Heurteaux, H.-J. Galla, T. Budde, H. Wiendl, S.G. Meuth, Endothelial TWIK-related potassium channel-1 (TREK1) regulates immune-cell trafficking into the CNS., Nat. Med. 19 (2013) 1161–1165.

[18] R.T. Holman, S.B. Johnson, E. Kokmen, Deficiencies of polyunsaturated fatty acids and replacement by nonessential fatty acids in plasma lipids in multiple sclerosis, Proc. Natl. Acad. Sci. U. S. A. 86 (1989) 4720–4724.

[19] P. Del Boccio, D. Pieragostino, M. Di Ioia, F. Petrucci, A. Lugaresi, G. De Luca, D. Gambi, M. Onofrj, C. Di Ilio, P. Sacchetta, A. Urbani, Lipidomic investigations for the characterization of circulating serum lipids in multiple sclerosis, J. Proteomics. 74 (2011) 2826–2836.

[20] J. Kurz, R. Brunkhorst, C. Foerch, L. Blum, M. Henke, L. Gabriel, T. Ulshöfer, N. Ferreirós, M.J. Parnham, G. Geisslinger, S. Schiffmann, The relevance of ceramides and their synthesizing enzymes for multiple sclerosis, Clin. Sci. 132 (2018) 1963–1976.

[21] O.G. Vidaurre, J.D. Haines, I. Katz Sand, K.P. Adula, J.L. Huynh, C.A. Mcgraw, F. Zhang, M. Varghese, E. Sotirchos, P. Bhargava, V.V.R. Bandaru, G. Pasinetti, W. Zhang, M. Inglese, P.A. Calabresi, G. Wu, A.E. Miller, N.J. Haughey, F.D. Lublin, P. Casaccia, Cerebrospinal fluid ceramides from patients with multiple sclerosis impair neuronal

bioenergetics, Brain. 137 (2014) 2271–2286.

[22] Y.Y. Zhao, X. long Cheng, R.C. Lin, Lipidomics Applications for Discovering Biomarkers of Diseases in Clinical Chemistry, Elsevier Inc., 2014.

[23] J. Lv, L. Zhang, F. Yan, X. Wang, Clinical lipidomics: a new way to diagnose human diseases, Clin. Transl. Med. 7 (2018) 10–12.

[24] C.H. Polman, S.C. Reingold, B. Banwell, M. Clanet, J.A. Cohen, M. Filippi, K. Fujihara, E. Havrdova, M. Hutchinson, L. Kappos, F.D. Lublin, X. Montalban, P. O'Connor, M. Sandberg-Wollheim, A.J. Thompson, E. Waubant, B. Weinshenker, J.S. Wolinsky, Diagnostic criteria for multiple sclerosis: 2010 Revisions to the McDonald criteria, Ann. Neurol. 69 (2011) 292–302.

[25] S. Anjos, E. Feiteira, F. Cerveira, T. Melo, A. Reboredo, S. Colombo, R. Dantas, E. Costa, A. Moreira, S. Santos, A. Campos, R. Ferreira, P. Domingues, M.R.M. Domingues, Lipidomics Reveals Similar Changes in Serum Phospholipid Signatures of Overweight and Obese Pediatric Subjects, J. Proteome Res. 18 (2019) 3174–3183.

[26] E.M. Bartlett, D.H. Lewis, Spectrophotometric determination of phosphate esters in the presence and absence of orthophosphate, Anal. Biochem. 36 (1970) 159–167.

[27] T. Pluskal, S. Castillo, A. Villar-Briones, ̃M. Oresĭc, MZmine 2: Modular Framework for Processing, Visualizing, and Analyzing Mass Spectrometry-Based Molecular Profile Data., BMC Bioinf. 11 (2010) 395.

[28] S. Colombo, T. Melo, M. Martínez-López, M.J. Carrasco, M.R. Domingues, D. Pérez-Sala, P. Domingues, Phospholipidome of endothelial cells shows a different adaptation response upon oxidative, glycative and lipoxidative stress, Sci. Rep. 8 (2018) 1–13.

[29] Y. V. Karpievitch, S.B. Nikolic, R. Wilson, J.E. Sharman, L.M. Edwards, Metabolomics data normalization with EigenMS, PLoS One. 9 (2014) 1–10.

[30] S. Le, J. Josse, F. Husson, FactoMineR: An R Package for Multivariate Analysis., J. Stat. Softw. 25 (2008) 1–18.

[31] A. Kassambara, F. Mundt, factoextra: Extract and Visualize the Results of Multivariate Data Analyses. R package version 1.0.7., (2020).

[32] R. Kolde, Kolde, R. Pheatmap: Pretty Heatmaps. R package version 1.0.12., (n.d.).

[33] H. Wickham, ggplot2 – Elegant Graphics for Data Analysis., 2nd Editio, Springer Nature, 2016.

[34] H. Wickham, R. François, L. Henry, K. Müller, dplyr: A Grammar of Data Manipulation. R package version 0.7.7., (2018).

[35] H. Wickham, L. Henry, tidyr: Easily Tidy Data with “spread()” and “gather()” Functions., (2018).

[36] M. Kuhn, caret: Classification and Regression Training. R package version 6.0-86., (2020).

[37] X. Robin, N. Turck, A. Hainard, N. Tiberti, F. Lisacek, J.-C. Sanchez, M. Müller, pROC: an open-source package for R and S+ to analyze and compare ROC curves, BMC Bioinformatics. 12 (2011) 77.

[38] N.M.S. Society, What is MS?, (2020). https://www.nationalmssociety.org/ (accessed March 16, 2020).

[39] P. Risé, S. Eligini, S. Ghezzi, S. Colli, C. Galli, Fatty acid composition of plasma, blood cells and whole blood: relevance for the assessment of the fatty acid status in humans, Prostaglandins Leukot. Essent. Fat. Acids. 76 (2007) 363–369.

[40] M.O. Trépanier, K.D. Hildebrand, S.D. Nyamoya, S. Amor, R.P. Bazinet, M. Kipp, Phosphatidylcholine 36:1 concentration decreases along with demyelination in the cuprizone animal model and in post-mortem multiple sclerosis brain tissue, J. Neurochem.

145 (2018) 504–515.

[41] I. Cicalini, C. Rossi, D. Pieragostino, L. Agnifili, L. Mastropasqua, M. di Ioia, G. De Luca, M. Onofrj, L. Federici, P. Del Boccio, Integrated Lipidomics and Metabolomics Analysis of Tears in Multiple Sclerosis: An Insight into Diagnostic Potential of Lacrimal Fluid, Int. J. Mol. Sci. 20 (2019) 1–16.

[42] P. Villoslada, C. Alonso, I. Agirrezabal, E. Kotelnikova, I. Zubizarreta, I. Pulido-Valdeolivas, A. Saiz, M. Comabella, X. Montalban, L. Villar, J.C. Alvarez-Cermeño, O. Fernández, R. Alvarez-Lafuente, R. Arroyo, A. Castro, Metabolomic signatures associated with disease severity in multiple sclerosis, Neurol. Neuroimmunol. NeuroInflammation. 4 (2017) 1–10.

[43] J. Vitallé, I. Terrén, A. Orrantia, O. Zenarruzabeitia, F. Borrego, CD300 receptor family in viral infections, Eur. J. Immunol. 49 (2019) 364–374.

[44] O. Zenarruzabeitia, J. Vitallé, C. Eguizabal, V.R. Simhadri, F. Borrego, The Biology and Disease Relevance of CD300a, an Inhibitory Receptor for Phosphatidylserine and Phosphatidylethanolamine, J. Immunol. 194 (2015) 5053–5060.

[45] L.A. O'Neill, R.J. Kishton, J. Rathmell, A guide to immuno-metabolism for immunologists., Nat Rev Immunol. 16 (2016) 553–565.

[46] A.M. Luoma, F. Kuo, O. Cakici, M.N. Crowther, A.R. Denninger, R.L. Avila, P. Brites, D.A. Kirschner, Plasmalogen phospholipids protect internodal myelin from oxidative damage., Free Radic Biol Med. 84 (2015) 296–310.

[47] S. Wallner, G. Schmitz, Plasmalogens the neglected regulatory and scavenging lipid species., Chem. Phys. Lipids. 164 (2011) 573–589.

[48] K.J. Smith, R. Kapoor, P.A. Felts, Demyelination: the role of reactive oxygen and nitrogen species., Brain Pathol. 9 (1999) 69–92.

[49] S. Aggarwal, L. Yurlova, M. Simons, Central nervous system myelin: structure, synthesis and assembly., Trends Cell Biol. 21 (2011) 585–593.

[50] O.H. Morand, R.A. Zoeller, C.R. Raetz, Disappearance of plasmalogens from membranes of animal cells subjected to photosensitized oxidation., J. Biol. Chem. 263 (1988) 11597–11606.

[51] R.A. Zoeller, O.H. Morand, C.R. Raetz, A possible role for plasmalogens in protecting animal cells against photosensitized killing., J. Biol. Chem. 263 (1988) 11590–11596.

[52] R. Padureanu, C.V. Albu, R.R. Mititelu, M.V. Bacanoiu, A.O. Docea, D. Calina, V. Padureanu, G. Olaru, R.E. Sandu, R.D. Malin, A.-M. Buga, Oxidative Stress and Inflammation Interdependence in Multiple Sclerosis, J. Clin. Med. 8 (2019) 1815.

[53] J. Qin, R. Goswami, R. Balabanov, G. Dawson, Oxidized Phosphatidylcholine Is a Marker for Neuroinflammation in Multiple Sclerosis Brain, J. Neurosci. Res. 85 (2007) 977–984.

[54] L. Haider, M.T. Fischer, J.M. Frischer, J. Bauer, R. Höftberger, G. Botond, H. Esterbauer, C.J. Binder, J.L. Witztum, H. Lassmann, Oxidative damage in multiple sclerosis lesions, Brain. 134 (2011) 1914–1924.

[55] T.M. Stulnig, J. Huber, N. Leitinger, E.M. Imre, P. Angelisová, P. Nowotny, W. Waldhäusl, Polyunsaturated Eicosapentaenoic Acid Displaces Proteins from Membrane Rafts by Altering Raft Lipid Composition, J. Biol. Chem. 276 (2001) 37335–37340.

[56] A. Monteiro, P. Rosado, L. Rosado, A.M. Fonseca, A. Paiva, Alterations in circulating T cell functional subpopulations in interferon-beta treated multiple sclerosis patients: A pilot study, J. Neuroimmunol. 339 (2020) 577113.

[57] A. Trotter, E. Anstadt, R.B. Clark, F. Nichols, A. Dwivedi, K. Aung, J.L. Cervantes, The role of phospholipase A2 in multiple Sclerosis: A systematic review and meta-analysis, Mult. Scler. Relat. Disord. 27 (2019) 206–213.

[58] E.M.L. De Oliveira, D.A. Montani, D. Oliveira-Silva, A.F. Rodrigues-Oliveira, S.L.D.A. Matas, G.B.P. Fernandes, I.D.C.G. Da Silva, E.G. Lo Turco, Multiple sclerosis has a distinct lipid signature in plasma and cerebrospinal fluid, Arq. Neuropsiquiatr. 77 (2019) 696–704.